



**Mobile Hotspot
FCC ID: PKRISGM2100**

**Band n260
Power Density Simulation Report**

August 3, 2020

Revision 2.2

Table of Contents

Contents

1 GENERAL	3
1.1 SCOPE	3
2 THEORY OF OPERATION	4
2.1 BEAM FORMING	4
2.0 TX DUTY CYCLE.....	4
3 SIMULATION METHODOLOGY	4
3.1 ELECTROMAGNETIC SIMULATION	4
3.1.1 Tool Description	4
3.1.2 Solver Description	5
3.1.3 Power Density Calculation	5
3.1.4 Power Averaging	6
3.1.5 3D Modeling	6
3.1.6 Antenna source excitation.....	7
3.1.7 Power Density evaluation planes	7
3.1.8 Simulation to Find worst case value	8
4 SIMULATION SETUP	9
4.1 SIMULATED SETUP OVER THE PRE-DEFINED PLANE	9
4.2 INPUT POWER.....	10
5 VALIDATION OF SIMULATION MODEL	10
5.1 COMPARISON BETWEEN SIMULATED AND MEASURED	10
5.2 SUMMARIZED SIMULATED PD VS MEASURED PD TEST RESULT	10
6 SIMULATION RESULTS	19
6.1 POWER DENSITY FOR BAND N260:.....	19
6.1.1 Ant-0 – Simulated Power Density	19
6.1.2 Ant-1 – Simulated Power Density	20
7 SUMMARY	21
7.1 UNCERTAINTY	21

1 General

1.1 Scope

This report is intended to support FCC compliance for the mobile hotspot using mm Wave antenna modules.

Per the location of the antenna modules inside the hotspot platform, the distance between the antenna to the body of an end user, at the closest contact point, will be in the near field.

Near field power density calculations were estimated using EM simulation that includes the antenna module embedded inside the hotspot 3D model. These results are documented in the following sections of this report.

To prove the validity of these results, we will show how the results of the simulations are well correlated, to lab measurements of the antenna module inside the hotspot platform, for transition field to far field distances, where the theoretical far field boundary is calculated for reference. The near field simulation results are also presented in this document.

Chapter 2 provides relevant background on the antenna module. Chapter 3 describes the simulation methodology to determine RF exposure (power density) levels. Chapter 4 describes simulation setup. Chapter 5 covers validation and correlation between simulation and lab measurements. Chapter 6 shows simulated PD results. Chapter 7 provides a summary of the RF-Exposure analysis.

2 Theory of Operation

2.1 Beam Forming

Due to the high path loss of the mmW signal travelling between the transmitting and receiving points, 5G communication can be achieved by employing antenna arrays with directionally high gain to compensate for the high path loss. Only one antenna module can be functional at any given time.

In the antenna module, such an electronic steering antenna array with approximately ± 45 -degree steering angles being used. Beam forming is used to find the right direction for setting both the Rx and Tx beam directions. Many individual beams can be formed from a single module. This is accomplished by changing polarization, phase, or combinations thereof.

The number of antenna ports of the antenna array module consists of 16 ports (4 for each patch antenna), 8 vertically polarized ports and 8 horizontally polarized ports, respectively. The antenna ports are controlled by SW. The phase, polarization and number of ports used can change. The ports are selected per the created “code book” and is custom for each product. The code book lists the phase, polarization, and combinations to be used for beamforming. In the 16 ports available in each patch antenna array, 8 ports are used to excite bands n257, n258 and n261, and 8 ports are used to excite band n260.

The ideal array structure is constructed to achieve the highest gain when the port combinations of the patch array elements are fed in phase to form a forward-looking high gain beam to the antenna origin (AZ, EL) = (0, 0).

2.0 Tx Duty Cycle

To capture worst-case power density conditions, simulations and measurements were performed assuming a 100% duty cycle. The TX-Duty-Cycle is established based on HW and FW implementation.

3 Simulation Methodology

3.1 Electromagnetic Simulation

3.1.1 Tool Description

For the EM simulation to calculate power density (PD) for mobile hotspot using qty. 2, mm Wave antenna modules, we use the commercially available ANSYS HFSS 2019 R3. ANSYS HFSS is widely used in industry for simulating 3D full-wave electromagnetic fields for antenna and RF radiation problem of high frequency component. ANSYS HFSS is implemented based on the Finite Element Method (FEM) operates in the frequency domain.

3.1.2 Solver Description

The HFSS tool is employing Finite Element Method in frequency domain to solve the EM fields in 3D space which is based on an accurate direct solver with first or second order basis functions. To start solving the problem, a volume containing the objects will be subdivided into electrically small regions that are called finite elements as the unknown functions. To subdivide system, the adaptive mesh method in HFSS is used. Then, HFSS starts to refine the initial mesh based on the designed wavelength and calculate the error for each iteration process with adaptive mesh refinement. The determination parameter of the number of iterations in HFSS is defined as convergence criteria, delta S, and the iterative adaptive mesh process repeats until the delta S is met. The accuracy of converged results depends on the delta S. The default setting in the HFSS for delta S is 2%. Fig. 1 is an example of final adaptive mesh of the antenna modules used in the simulation.

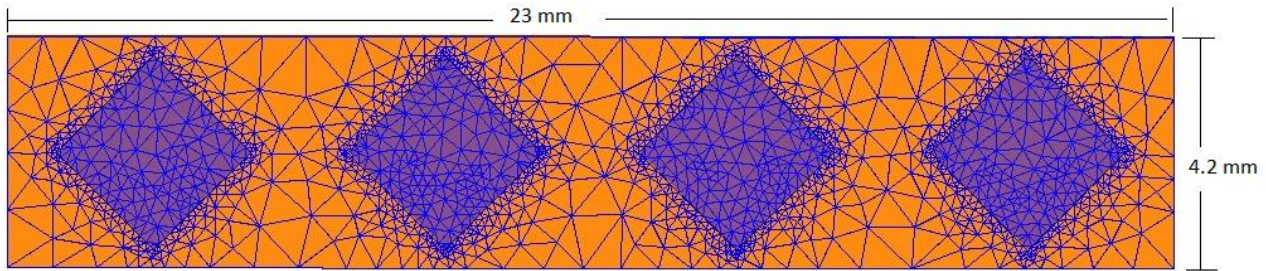


Fig. 1 Example of the adaptive mesh used in HFSS

3.1.3 Power Density Calculation

After simulation, HFSS can generate the electric and magnetic fields in each surface. For power density calculation, the electric field (\vec{E}) and magnetic field (\vec{H}) are needed. The actual consumption power can be expressed as the real part of the Poynting vector (\vec{P}) from the cross product of \vec{E} and the complex conjugation of \vec{H} as shown below:

$$\vec{P} = \frac{1}{2} \text{Re}(\vec{E} \times \vec{H}^*) \quad (1)$$

\vec{P} can be expressed as the localized power density based on a peak value of each spatial point on mesh grids and obtained directly from ANSYS HFSS simulation results. From the localized power density, the average power density can be evaluated over a 4 cm² square on any surfaces. The power density is calculated in the relevant plan (10 mm away from the hotspot plastic housing) over a surface of 4 cm² square.

3.1.4 Power Averaging

After the simulation has completed the E and H fields, power density can be calculated for the predefined surfaces. The figure shown below is an example of the power density for an antenna module at a predefined surface

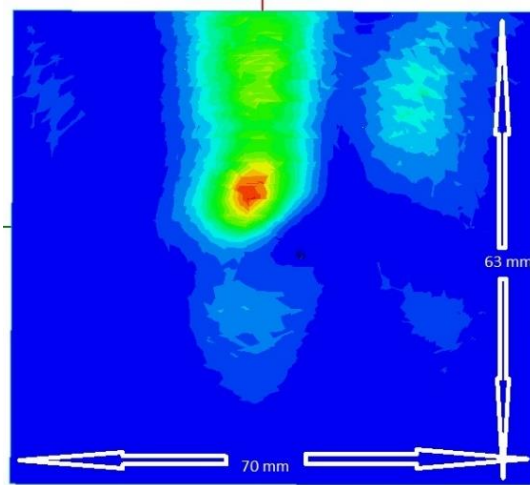


Fig. 2 – Example of calculated power density from HFSS

3.1.5 3D Modeling

Figure 3 shows the 3D simulation model using mm Wave antenna modules. The simulation modeling includes all the major components of the hotspot. These include items such as the Housing, PCB, metal antenna holder, display, touch panel, battery, legacy antennas and antenna modules Ant-0, Ant-1. Their material properties are shown in table 1.

Table 1 – Material Properties

Model Components	Dielectric Material	Dielectric Constant	Loss Tangent
Display, Heatsink, RJ45 & Shields	Aluminum	1.0	0
Battery & Touch Screen	Copper	1.0	0
PCB	FR4	4.4	0.2
Touch Panel Glass	Glass	5.5	0
Battery Door, Top & Bottom Housings	PC/ABS	2.85	0.0035

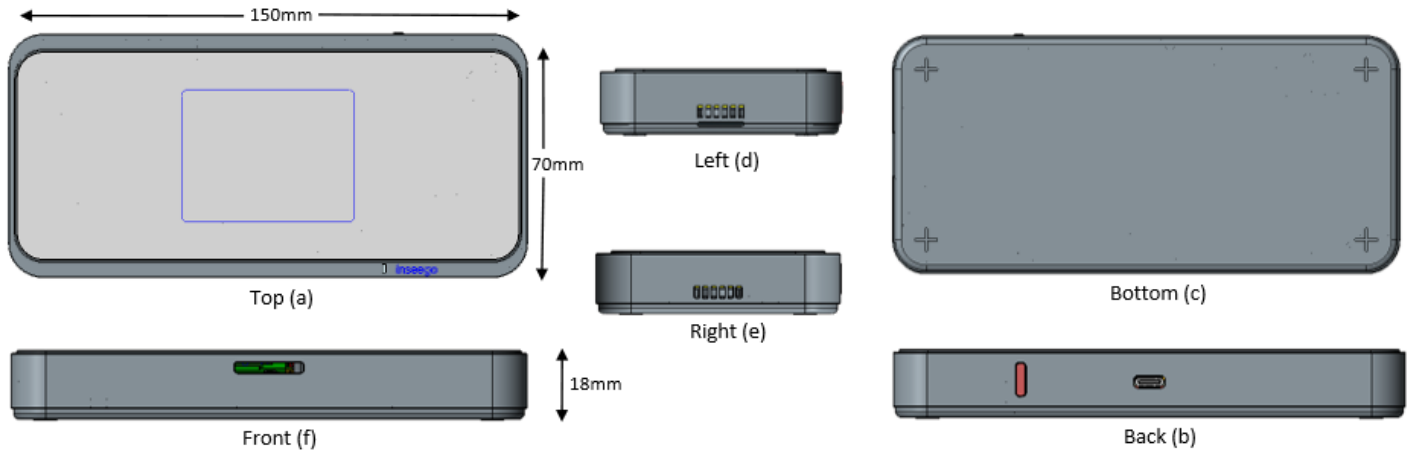


Fig. 3 – 3D model details

Both antenna modules are mounted above the PCB top layer and legacy antennas around the perimeter of the housing. Per figure 3, the antenna modules are positioned in the following way, Ant-0 faces the left side (d), Ant-1 faces the front side (f)

3.1.6 Antenna source excitation

The number of ports of each antenna module consists of 16 ports. The antenna is divided into 16 ports for the 1x4 patch array. 4 ports included in each patch element, 4 ports are divided into 2 vertical polarization, and 2 ports are horizontal polarization feeding. The patch array antenna consists of 4 patch elements. Each uses four ports as a source excitation. The input power and phase of each port are fed according to the “Code Book” when in operation.

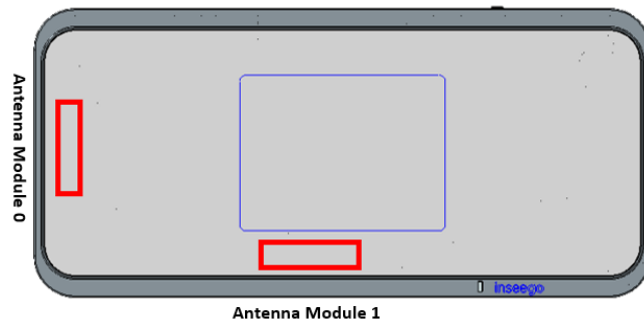


Fig. 4 – Simulation model showing the mounted locations of the antenna modules

3.1.7 Power Density evaluation planes

Table 2 shows the PD evaluation planes for each antenna module and Figures 5 and 5b illustrate the PD evaluation planes and truncation areas of the simulation model which are used to find the worst-case beamforming cases. Each antenna module is individually evaluated for worst case PD using multiple evaluation planes. These planes, S1 through S8, are positioned 10mm away from the hotspot surface. All the material properties used in the simulation model are chosen to be as close to the real device.

Table 2 - PD Simulation evaluation planes

Antenna Module	TOP	BOTTOM	FRONT	RIGHT	LEFT
0	S1	S3	S2	S5	S4
1	S6	S8	S7	X	X

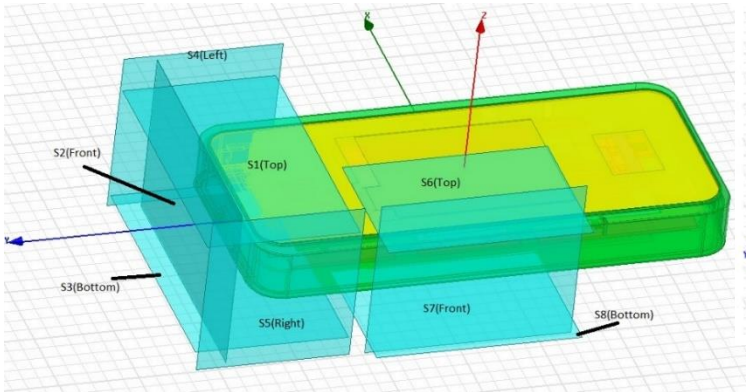


Fig. 5 – power density evaluation planes and truncation areas

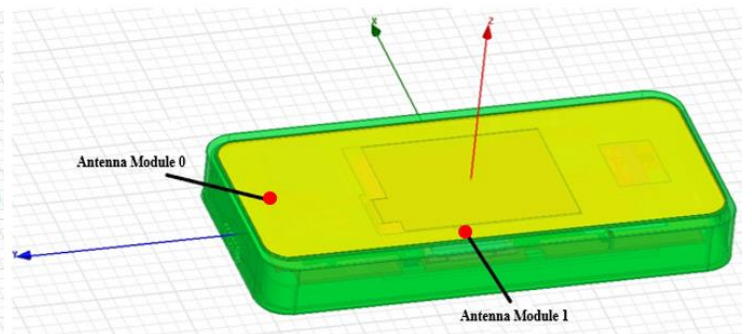


Fig. 5b – antenna modules in simulation model

3.1.8 Simulation to Find worst case value

To find the maximum power density value, firstly, power density is calculated and displayed on all evaluation surfaces. The power concentration areas for each evaluation surface are then identified. Second, a 2 cm x 2 cm square plane is moved in both X and Y directions across the entire surface and power density is calculated for each location. Third, the resulted maximum power density is divided by the area of the plane to get the average maximum power density over the 2 cm x 2 cm square area.

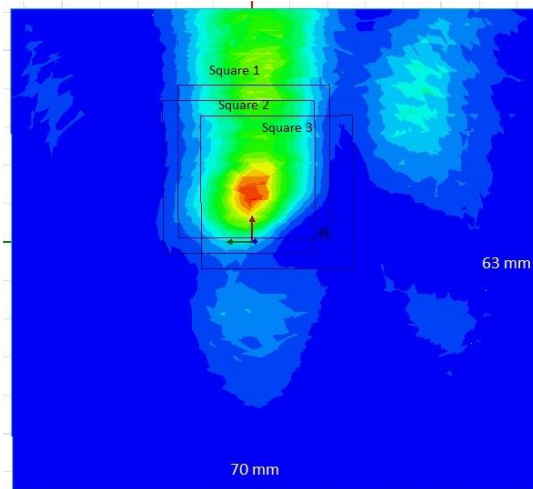


Fig. 6 – maximum value of average power density

Fig. 6 shows three 2 cm x 2 cm squares, square 1, 2 and 3, positioned over the highest power density areas. These areas are obtained from the simulation results and illustrates the process of locating the area of highest average power density.

4 Simulation Setup

4.1 Simulated Setup over the Pre-defined Plane

From the E-Field and H-Field generated by simulations, we can calculate the local power density by employing Poynting theorem. Figure 7 shows the local power density of the computed complex E-field and H-field for the worst case in the pre-defined plane surface. The excited power for the antenna module is set to maximum input power for each active port. A 4cm^2 square can then be placed around the high intensity zones to find the worst case of average power density as shown in above Figure 6.

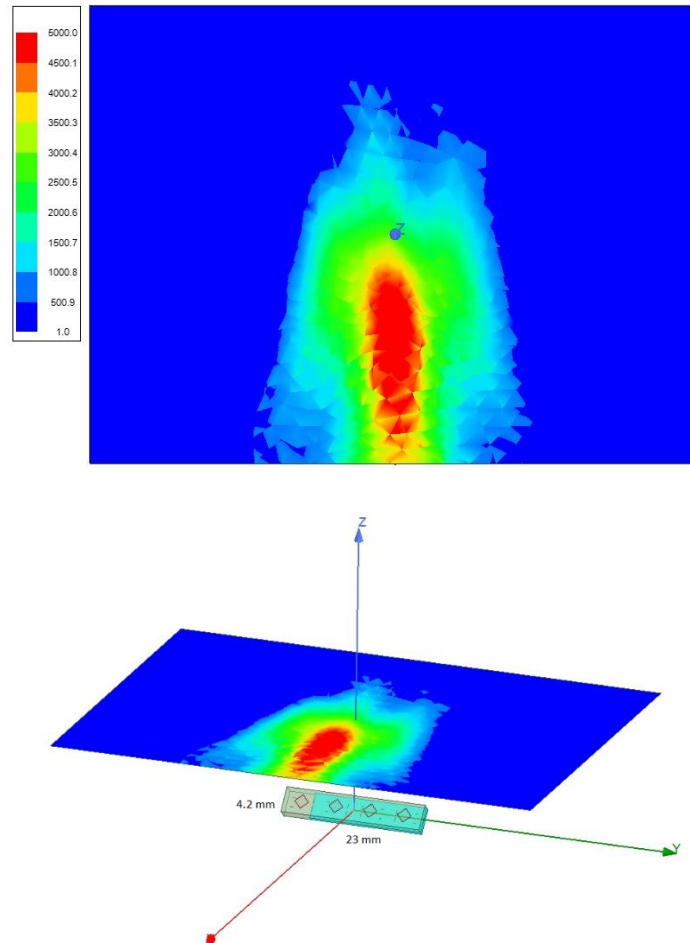


Fig. 7 - Local power density at pre-defined surface plane

Figure 7 shows an example of the simulated power density at a 10 mm distance from the top surface. Due to the time-consuming method used in measuring near field power density in the mm Wave spectrum, the most practical method is to use simulation results to find the antenna beam and surface with worst-case power density. Once the surface and beam are located, the power density measurements are performed on the worst-case power density surface or surfaces.

4.2 Input Power

Table 3 shows the input powers used for each active port for both Simulation and Measurement. For measurements, the hotspot is configured to Factory Test Mode and input power values are entered via SW for each active port. For simulations, these values were entered directly into the HFSS setup parameters.

Table 3 – Measured and Simulated input powers used for each active port

Mode/Band	Antenna	Input Power (dBm) SISO	Input Power (dBm) MIMO
5G NR n260	0	6	6
	1	6	6

5 Validation of Simulation Model

5.1 Comparison between Simulated and Measured

The beam characterization code book provides the relative phase between each input port of the antenna module and therefore defines all beams formed in real-world operation. Simulated and measured power density distributions for the antenna modules are shown in the below data. Based on these comparisons, the simulated and measured power densities have good correlation. Measurement uncertainty in mm Wave frequency simulation has measurement inaccuracy for material properties and are considered as error factors. Validation of simulations were measured in FTM (Factory Test Mode).

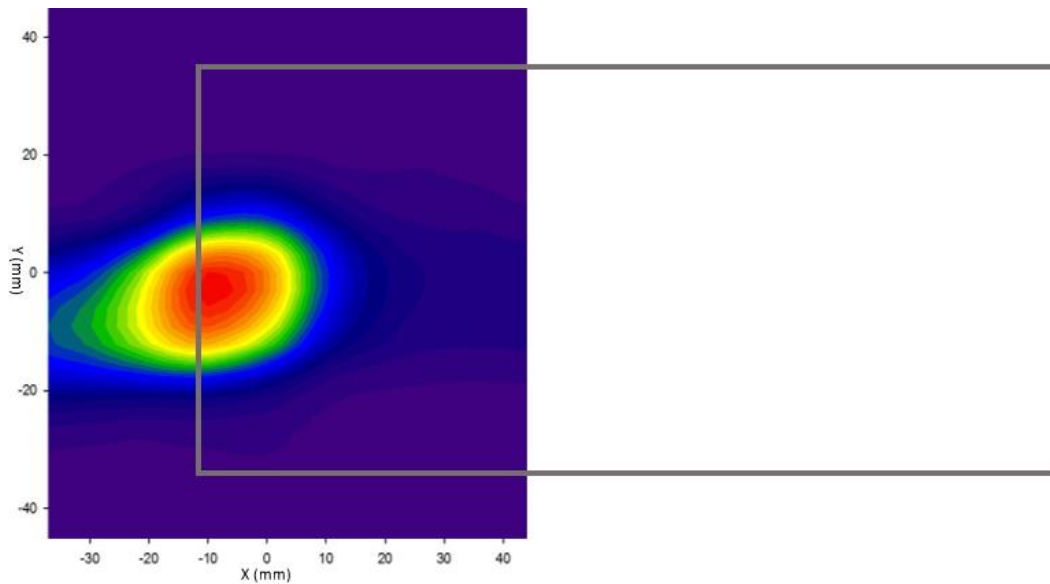
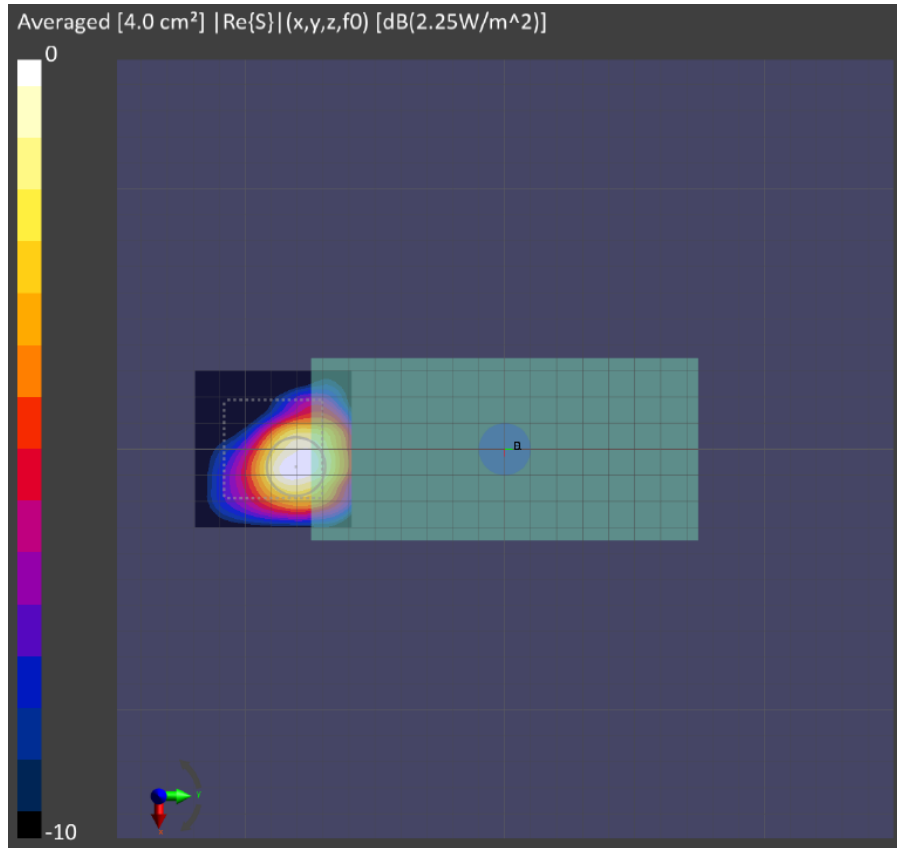
Edges were not required to be evaluated for Power Density if these edges were greater than 2.5 cm from the transmitting antenna according to FCC KDB Publication 941225 D06v02r01 Section III.

5.2 Summarized Simulated PD vs Measured PD Test Result

Power Density 4cm2 avg. PD (mW/cm2)											
Band	Surface Side	Surface ID	Polarization	Element Type	Freq. GHz	Channel	Antenna	Beam ID	Measured mW/cm ²	Simulated mW/cm ²	Sim. vs Meas. (mW/cm ²) Δ dB
n260	Top	S1	H	Patch	38.500	Mid	0	28	0.225	0.844	5.74
	Top	S1	V	Patch	38.500	Mid		149	0.114	0.684	7.78
	Front	S2	H	Patch	38.500	Mid		29	0.193	0.668	5.39
	Front	S2	V	Patch	38.500	Mid		154	0.131	0.804	7.88
	Top	S6	H	Patch	38.500	Mid	1	22	0.202	0.992	6.91
	Top	S6	V	Patch	38.500	Mid		140	0.176	1.048	7.75
	Front	S7	H	Patch	38.500	Mid		16	0.262	0.784	4.76
	Front	S7	V	Patch	38.500	Mid		140	0.153	0.812	7.25

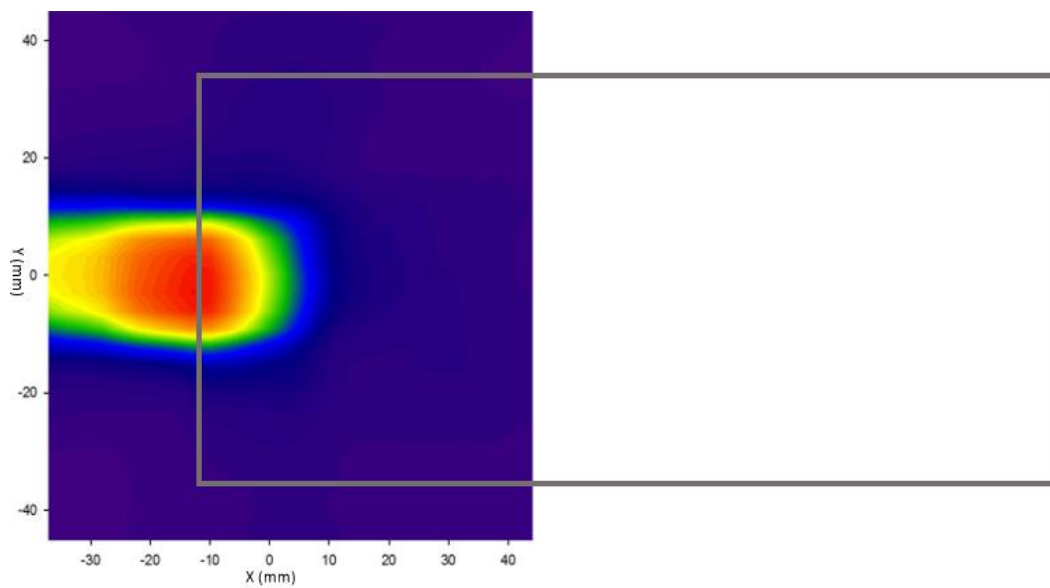
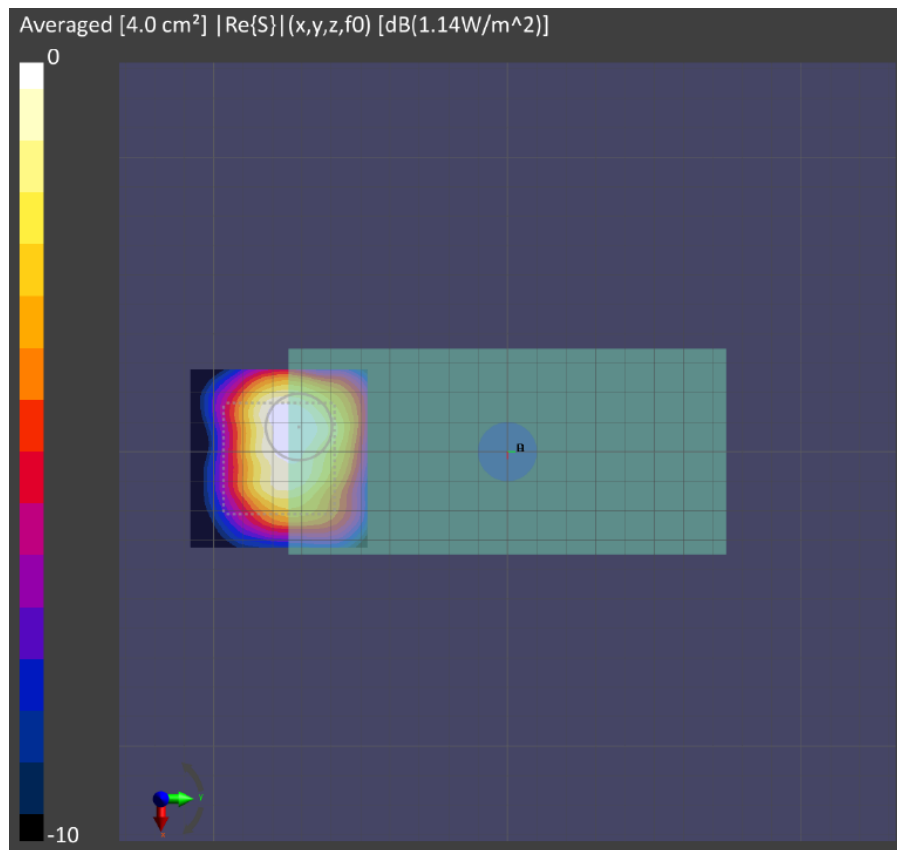
4cm2 Averaged Power Density

- ANT-0: Top Surface (S1), Mid Channel, H-Pol, Beam ID 28



4cm2 Averaged Power Density

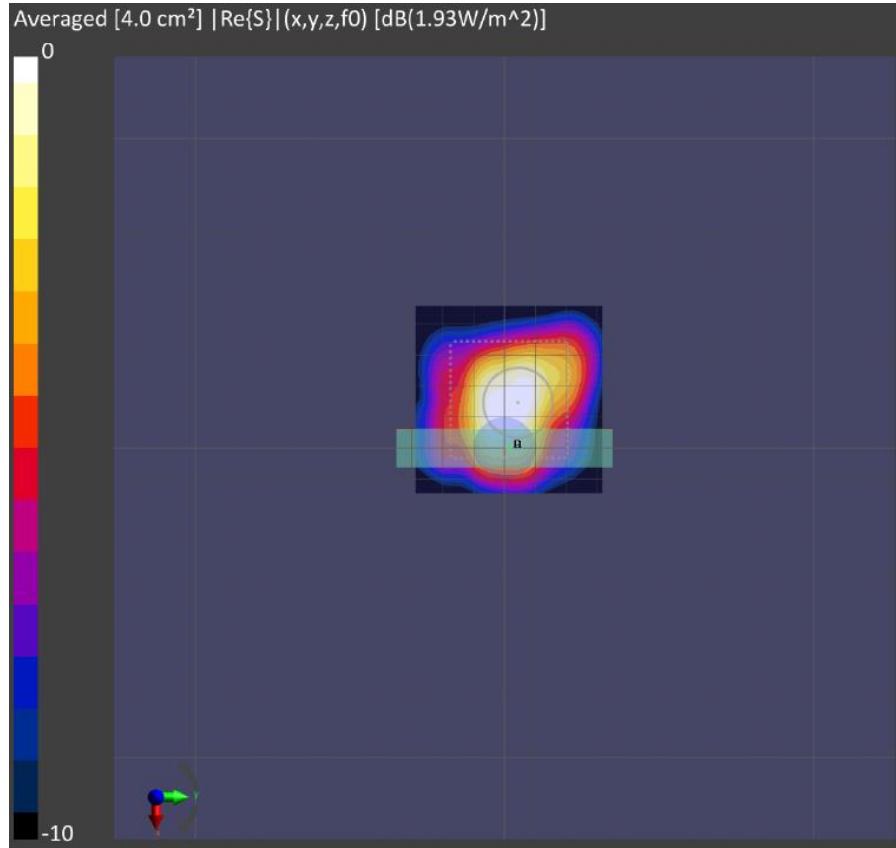
- ANT-0: Top Surface (S1), Mid Channel, V-Pol, Beam ID 149



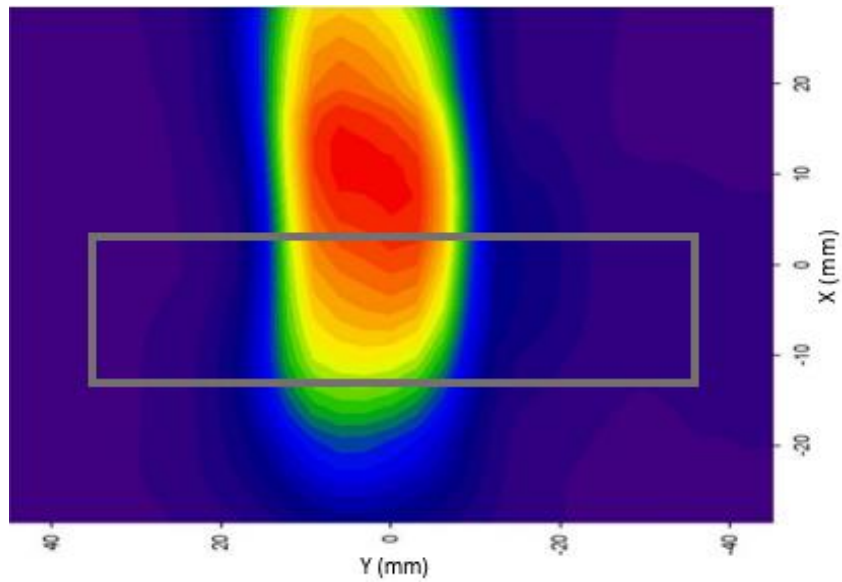
(b) Simulation

4cm2 Averaged Power Density

- ANT-0: Front Surface (S2), Mid Channel, H-Pol, Beam ID 29



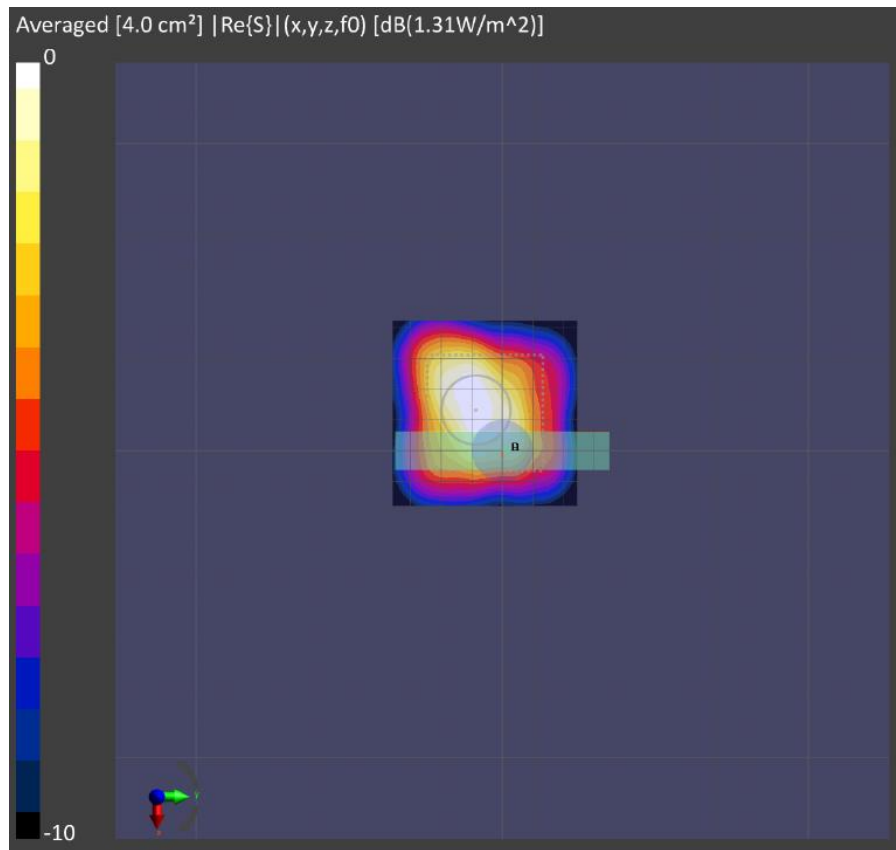
(a) Measurement



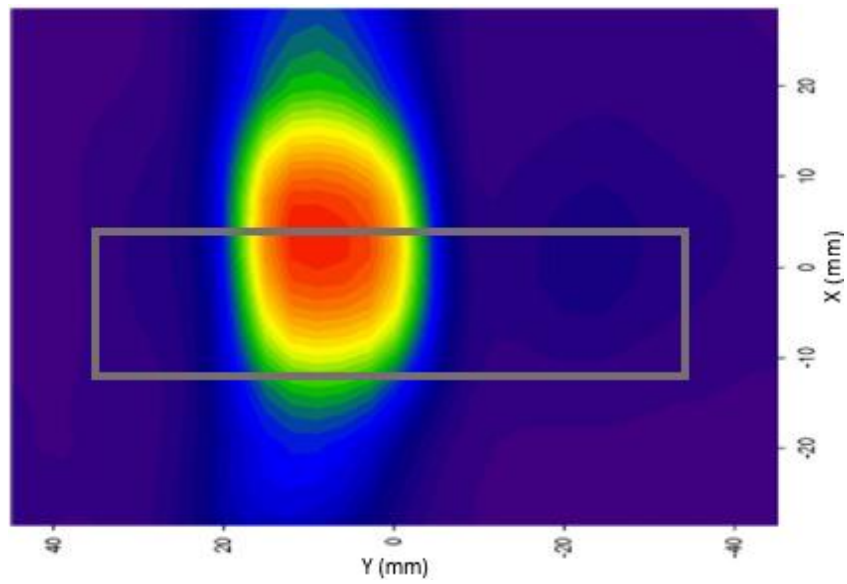
(b) Simulation

4cm2 Averaged Power Density

- ANT-0: Front Surface (S2), Mid Channel, V-Pol, Beam ID 154



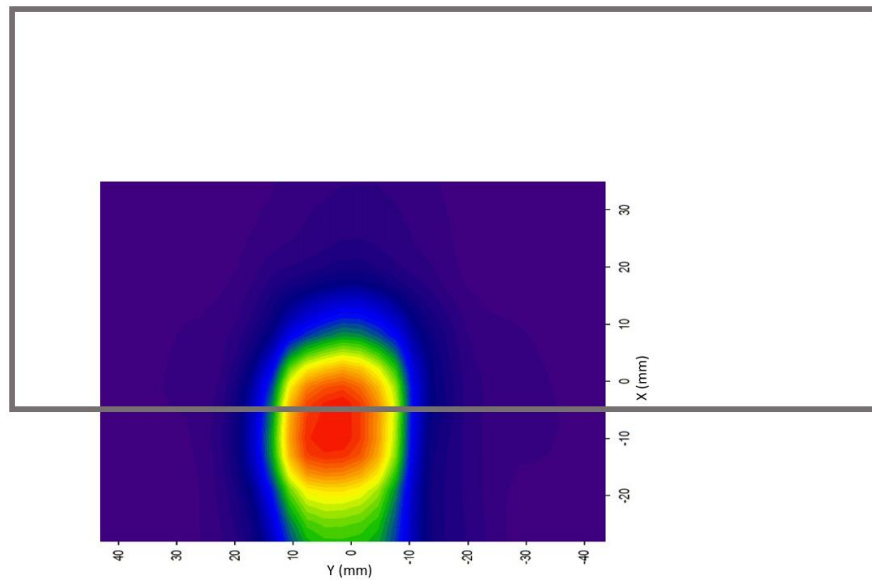
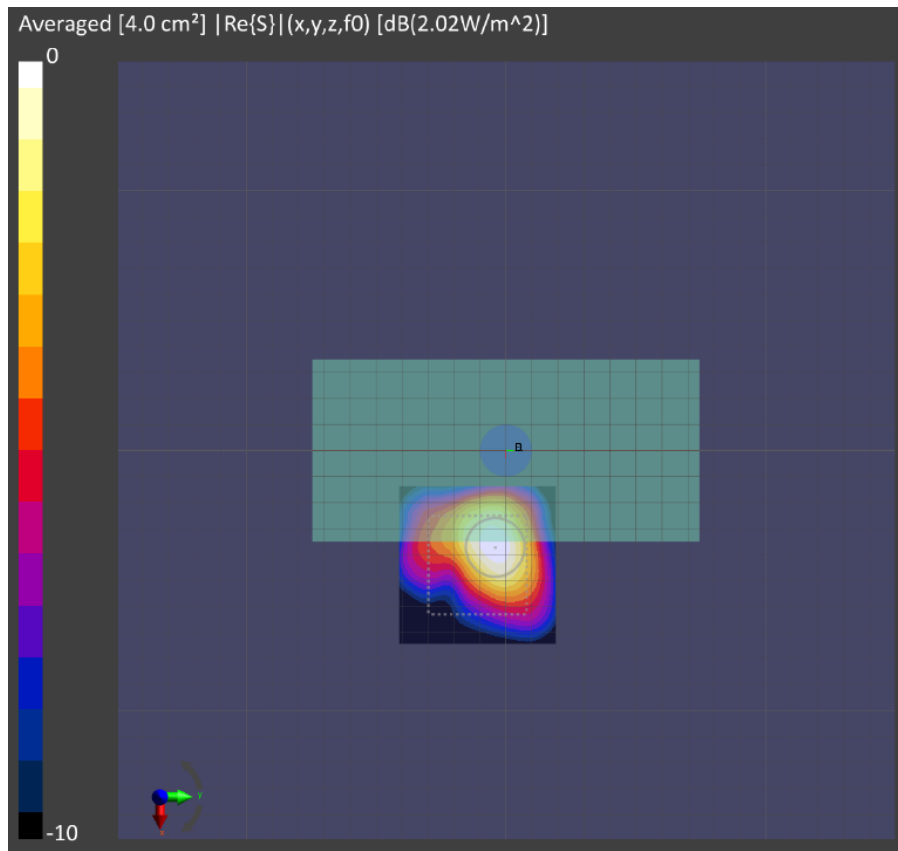
(a) Measurement



(b) Simulation

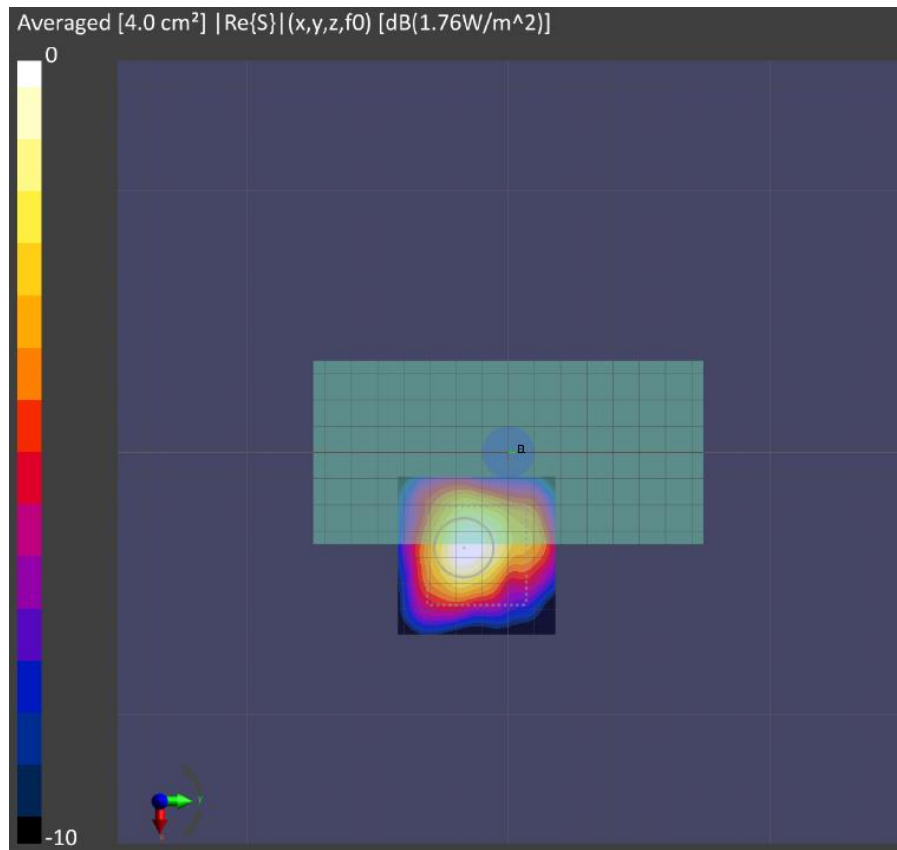
4cm2 Averaged Power Density

- ANT-1: Top Surface (S6), Mid Channel, H-Pol, Beam ID 22

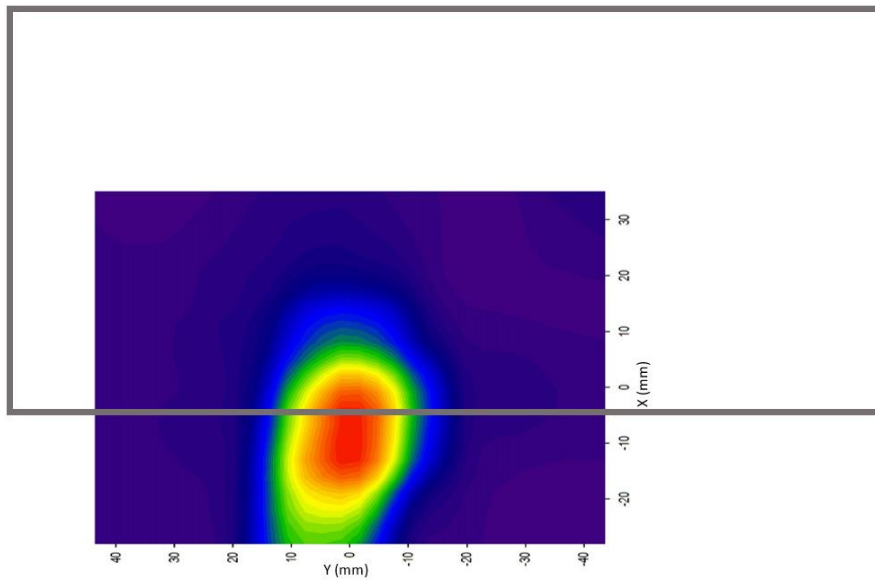


4cm2 Averaged Power Density

- ANT-1: Top Surface (S6), Mid Channel, V-Pol, Beam ID 140



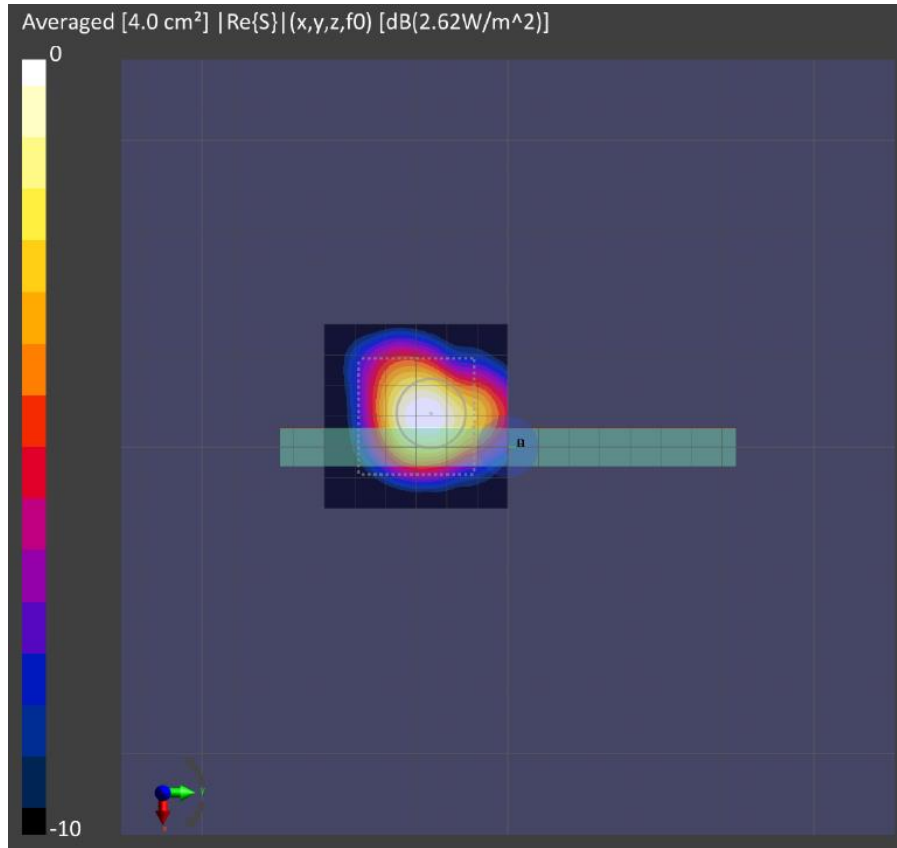
(a) Measurement



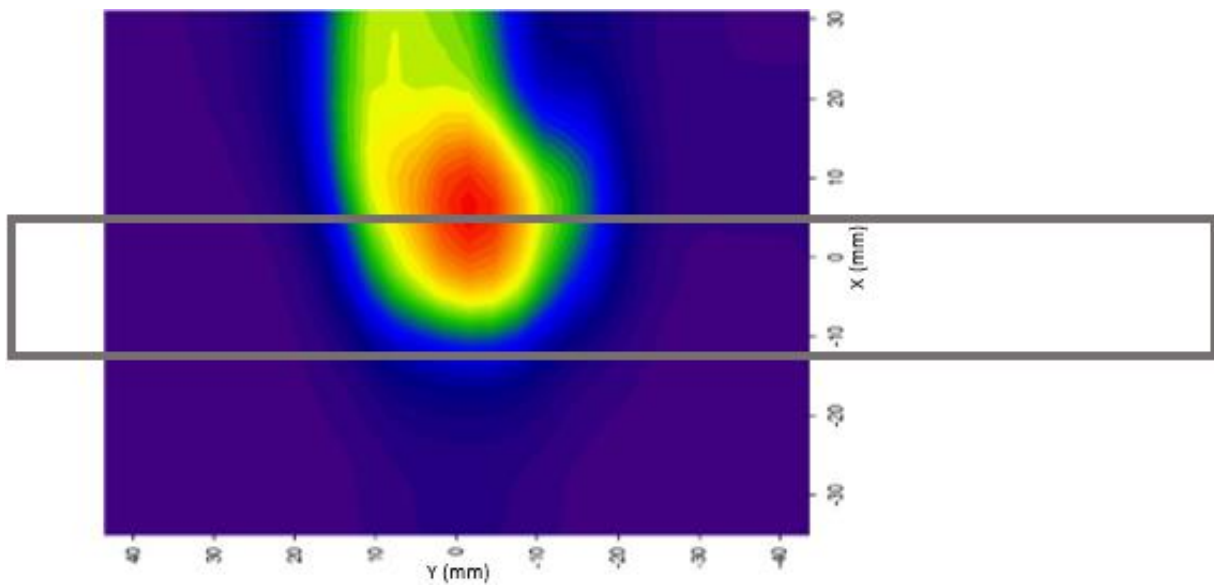
(b) Simulation

4cm2 Averaged Power Density

- ANT-1: Front Surface (S7), Mid Channel, H-Pol, Beam ID 16



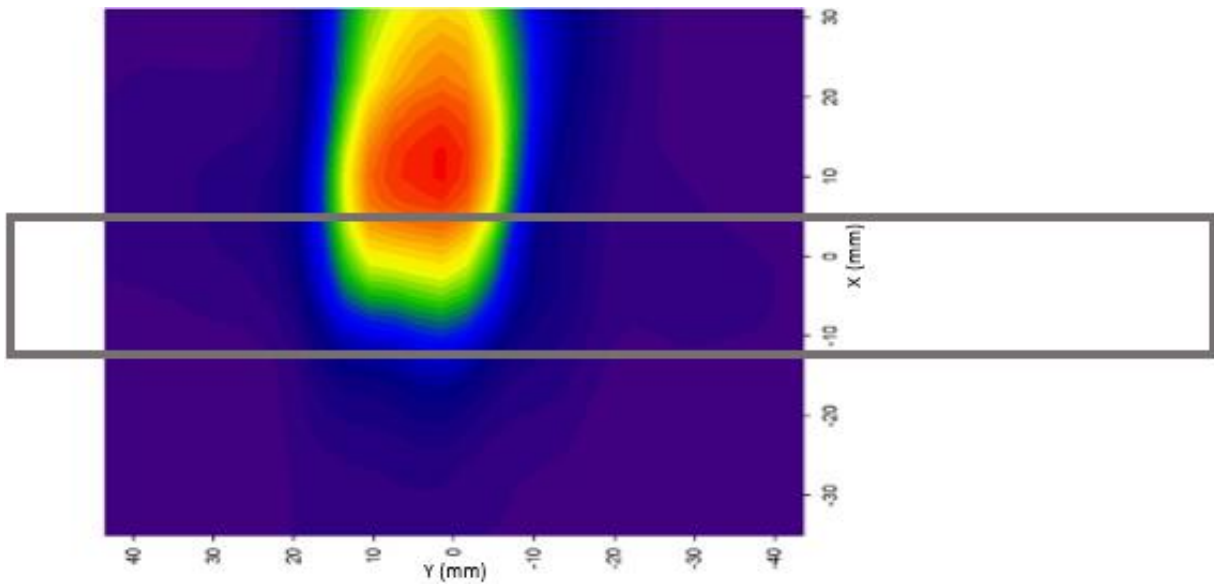
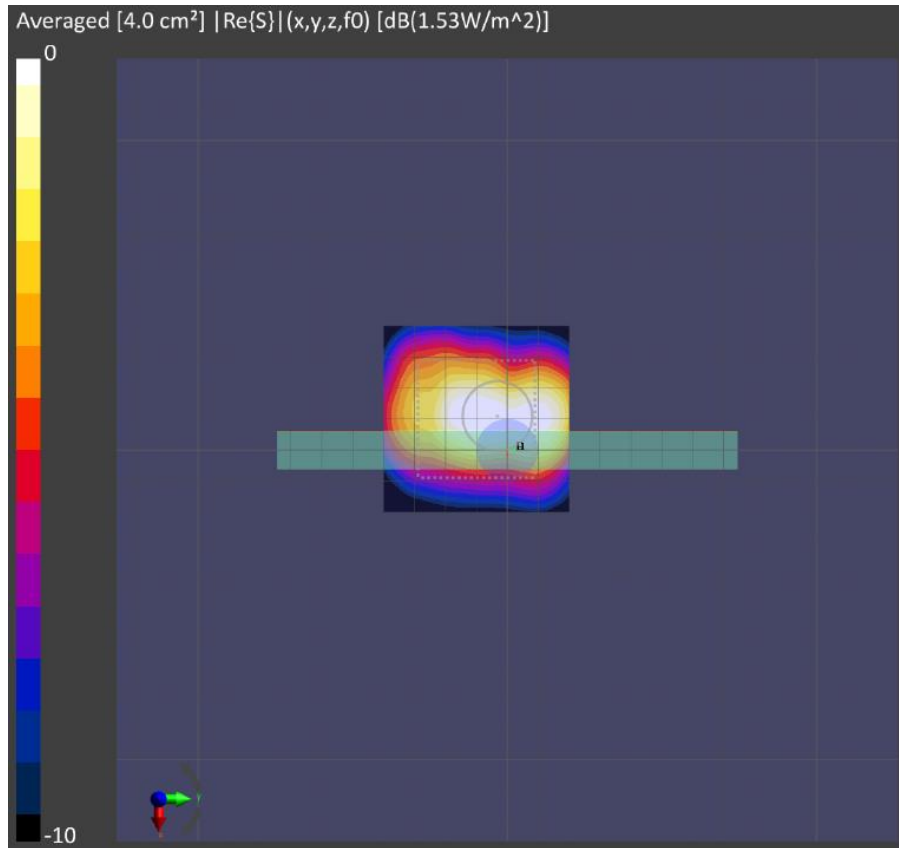
(a) Measurement



(b) Simulation

4cm2 Averaged Power Density

- ANT-1: Front Surface (S7), Mid Channel, V-Pol, Beam ID 140



6 Simulation Results

6.1 Power Density for Band n260:

Table 4 & 5 show the PD simulations of Ant 0 and Ant 1 for evaluation surface planes specified in Table 2.
 Band n260 Simulation Frequencies: Low 37.00GHz, Mid 38.50GHz, High 40.00GHz

6.1.1 Ant-0 – Simulated Power Density

Table 4 – PD Simulations

n260 PD Simulation					(S1) Top Surface			(S3) Bottom Surface			(S2) Front Surface			(S4) Left Surface			(S5) Right Surface								
Ant Module	Ant. Type	SISO/MIMO & Polarization	Feed no.	Beam ID	4cm2 avg. PD (mW/cm2) @ 10mm distance																				
					Channel																				
					Low	Mid	High	Low	Mid	High	Low	Mid	High	Low	Mid	High	Low	Mid	High	Low	Mid	High			
0	Patch	Single Beam H-pol	1	1	0.118	0.150	0.137	0.015	0.027	0.047	0.121	0.160	0.164	0.009	0.009	0.006	0.009	0.012	0.030						
			2	5	0.344	0.322	0.302	0.060	0.070	0.070	0.286	0.364	0.308	0.012	0.006	0.008	0.026	0.054	0.058						
			2	6	0.366	0.444	0.336	0.066	0.086	0.104	0.294	0.242	0.212	0.018	0.034	0.046	0.016	0.010	0.018						
			2	7	0.348	0.338	0.344	0.064	0.056	0.064	0.316	0.416	0.382	0.018	0.008	0.010	0.024	0.048	0.056						
			2	10	0.310	0.294	0.236	0.046	0.072	0.116	0.172	0.210	0.220	0.030	0.030	0.014	0.036	0.054	0.078						
			2	11	0.284	0.324	0.344	0.060	0.078	0.108	0.344	0.462	0.482	0.030	0.016	0.012	0.016	0.026	0.032						
			4	17	0.708	0.592	0.600	0.132	0.144	0.148	0.572	0.492	0.500	0.016	0.024	0.024	0.064	0.096	0.176						
			4	18	0.396	0.412	0.404	0.140	0.188	0.188	0.368	0.520	0.448	0.124	0.092	0.044	0.076	0.068	0.040						
			4	19	0.624	0.700	0.540	0.080	0.112	0.140	0.504	0.416	0.388	0.032	0.028	0.044	0.064	0.060	0.044						
			4	20	0.652	0.780	0.608	0.176	0.220	0.248	0.628	0.640	0.540	0.024	0.040	0.060	0.048	0.048	0.108						
			4	21	0.764	0.792	0.680	0.168	0.196	0.192	0.692	0.584	0.520	0.024	0.040	0.048	0.056	0.064	0.152						
			4	26	0.564	0.496	0.484	0.100	0.132	0.192	0.400	0.428	0.392	0.036	0.032	0.028	0.100	0.140	0.152						
			4	27	0.588	0.440	0.416	0.104	0.204	0.204	0.424	0.496	0.448	0.092	0.092	0.060	0.036	0.076	0.060						
			4	28	0.732	0.844	0.660	0.200	0.216	0.240	0.668	0.656	0.556	0.024	0.044	0.068	0.060	0.068	0.128						
			4	29	0.764	0.824	0.652	0.172	0.236	0.208	0.712	0.668	0.552	0.024	0.036	0.072	0.060	0.092	0.116						
			0	Patch	Single Beam V-pol	1	129	0.133	0.136	0.146	0.020	0.028	0.047	0.118	0.152	0.162	0.008	0.013	0.030	0.013	0.011	0.005			
						2	133	0.372	0.338	0.382	0.092	0.084	0.096	0.344	0.294	0.298	0.026	0.032	0.030	0.012	0.030	0.026			
						2	134	0.328	0.238	0.312	0.056	0.084	0.056	0.218	0.222	0.224	0.048	0.070	0.058	0.026	0.010	0.018			
						2	135	0.380	0.372	0.434	0.080	0.054	0.086	0.334	0.236	0.304	0.020	0.030	0.014	0.022	0.028	0.024			
						2	138	0.218	0.248	0.228	0.060	0.064	0.060	0.190	0.178	0.136	0.040	0.026	0.026	0.034	0.036	0.046			
						2	139	0.408	0.324	0.446	0.064	0.050	0.060	0.334	0.252	0.286	0.034	0.056	0.044	0.014	0.018	0.016			
						4	145	0.624	0.628	0.664	0.196	0.240	0.240	0.680	0.792	0.648	0.032	0.044	0.032	0.056	0.044	0.060			
						4	146	0.504	0.540	0.596	0.152	0.192	0.244	0.608	0.656	0.564	0.036	0.072	0.064	0.124	0.056	0.072			
						4	147	0.592	0.432	0.496	0.200	0.304	0.028	0.408	0.400	0.364	0.120	0.196	0.164	0.084	0.044	0.020			
						4	148	0.800	0.668	0.752	0.196	0.156	0.192	0.640	0.492	0.640	0.056	0.084	0.080	0.024	0.040	0.040			
						4	149	0.724	0.684	0.784	0.224	0.152	0.228	0.664	0.520	0.640	0.060	0.100	0.096	0.028	0.040	0.032			
						4	154	0.592	0.592	0.640	0.184	0.248	0.244	0.664	0.804	0.616	0.044	0.044	0.044	0.052	0.044	0.064			
						4	155	0.444	0.452	0.444	0.188	0.236	0.168	0.520	0.576	0.504	0.092	0.068	0.072	0.108	0.084	0.048			
						4	156	0.728	0.544	0.640	0.100	0.188	0.184	0.580	0.444	0.476	0.100	0.172	0.168	0.024	0.028	0.028			
		4				157	0.752	0.664	0.792	0.196	0.164	0.228	0.640	0.504	0.640	0.064	0.096	0.096	0.028	0.040	0.032				
		0				Patch	Paired Beam	1	1	129	0.108	0.119	0.113	0.021	0.023	0.033	0.147	0.145	0.161	0.011	0.016	0.021	0.008	0.011	0.023
								2	5	133	0.200	0.212	0.366	0.072	0.066	0.048	0.390	0.344	0.324	0.012	0.016	0.018	0.020	0.030	0.042
								2	6	134	0.274	0.294	0.266	0.036	0.056	0.054	0.180	0.134	0.188	0.026	0.032	0.050	0.022	0.016	0.016
			2	7	135			0.072	0.056	0.716	0.042	0.039	0.045	0.252	0.232	0.292	0.032	0.026	0.016	0.008	0.030	0.014			
			2	10	138			0.374	0.376	0.352	0.064	0.070	0.054	0.142	0.190	0.204	0.022	0.036	0.030	0.008	0.014	0.010			
			2	11	139			0.348	0.280	0.348	0.054	0.054	0.054	0.202	0.156	0.212	0.060	0.052	0.030	0.008	0.018	0.014			
			4	17	145			0.744	0.736	0.780	0.176	0.096	0.112	0.540	0.484	0.504	0.028	0.040	0.032	0.056	0.056	0.040			
			4	18	146			0.520	0.564	0.600	0.156	0.192	0.240	0.476	0.668	0.540	0.096	0.092	0.060	0.020	0.032	0.016			
			4	19	147			0.368	0.440	0.316	0.072	0.092	0.124	0.016	0.252	0.232	0.060	0.092	0.120	0.056	0.028	0.032			
			4	20	148			0.736	0.800	0.952	0.168	0.088	0.156	0.524	0.504	0.640	0.060	0.052	0.064	0.024	0.028	0.028			
			4	21	149			0.780	0.760	0.656	0.184	0.244	0.024	0.856	0.744	0.720	0.044	0.068	0.084	0.028	0.040	0.068			
			4	26	154			0.680	0.716	0.828	0.140	0.132	0.096	0.312	0.484	0.420	0.044	0.048	0.044	0.036	0.072	0.064			
			4	27	155			0.364	0.484	0.532	0.140	0.212	0.220	0.400	0.532	0.528	0.088	0.092	0.076	0.036	0.048	0.024			
			4	28	156			0.580	0.608	0.424	0.128	0.128	0.184	0.560	0.532	0.412	0.064	0.120	0.116	0.028	0.060	0.092			
			4	29	157			0.768	0.320	0.820	0.156	0.152	0.220	0.540	0.568	0.608	0.064	0.092	0.013	0.016	0.032	0.024			

6.1.2 Ant-1 – Simulated Power Density

Table 5 – PD Simulations

n260 PD Simulation					(S6) Top Surface			(S8) Bottom Surface			(S7) Front Surface			
Ant Module	Ant. Type	SISO/MIMO & Polarization	Feed no.	Beam ID	4cm2 avg. PD (mW/cm2) @ 10mm distance									
					Channel									
					Low	Mid	High	Low	Mid	High	Low	Mid	High	
1	Patch	Single Beam H-pol	1	0	0.217	0.282	0.200	0.009	0.010	0.013	0.155	0.173	0.116	
			2	2	0.470	0.738	0.580	0.016	0.024	0.018	0.378	0.478	0.324	
			2	3	0.352	0.466	0.488	0.016	0.038	0.020	0.298	0.402	0.476	
			2	4	0.444	0.386	0.398	0.024	0.032	0.026	0.358	0.524	0.388	
			2	8	0.492	0.484	0.446	0.028	0.030	0.030	0.400	0.426	0.344	
			2	9	0.440	0.342	0.342	0.020	0.034	0.026	0.302	0.432	0.334	
			4	12	0.952	0.976	0.916	0.040	0.072	0.060	0.804	0.756	0.684	
			4	13	0.692	0.620	0.560	0.040	0.048	0.048	0.468	0.476	0.616	
			4	14	0.644	0.760	0.804	0.032	0.044	0.076	0.444	0.556	0.524	
			4	15	0.592	0.860	0.668	0.036	0.044	0.052	0.428	0.552	0.600	
			4	16	0.812	0.816	0.828	0.044	0.076	0.048	0.684	0.784	0.616	
			4	22	0.928	0.992	0.936	0.052	0.064	0.064	0.744	0.744	0.676	
			4	23	0.788	0.840	0.808	0.048	0.048	0.040	0.524	0.668	0.640	
			4	24	0.696	0.708	0.644	0.040	0.044	0.044	0.416	0.532	0.400	
			4	25	0.704	0.808	0.792	0.040	0.068	0.036	0.576	0.696	0.676	
			Single Beam V-pol	1	128	0.217	0.275	0.213	0.007	0.008	0.010	0.250	0.173	0.124
				2	130	0.524	0.708	0.540	0.018	0.032	0.044	0.528	0.410	0.274
				2	131	0.328	0.364	0.336	0.016	0.016	0.020	0.278	0.246	0.256
				2	132	0.316	0.282	0.332	0.018	0.032	0.018	0.256	0.268	0.318
				2	136	0.330	0.448	0.502	0.020	0.026	0.028	0.450	0.492	0.528
				2	137	0.404	0.526	0.454	0.020	0.032	0.018	0.432	0.486	0.342
				4	140	0.748	1.048	0.844	0.064	0.064	0.060	0.952	0.812	0.572
				4	141	0.496	0.784	0.704	0.032	0.044	0.052	0.584	0.636	0.588
				4	142	0.696	0.716	0.672	0.044	0.060	0.044	0.708	0.512	0.592
				4	143	0.896	0.900	0.880	0.044	0.076	0.068	1.104	0.708	0.640
		4		144	0.572	0.580	0.688	0.048	0.072	0.068	0.776	0.600	0.572	
		4		150	0.736	0.976	0.832	0.052	0.056	0.064	0.920	0.760	0.672	
		4		151	0.832	0.804	0.592	0.044	0.076	0.044	0.816	0.492	0.484	
		4		152	0.904	0.876	0.856	0.048	0.088	0.076	1.088	0.776	0.616	
		4		153	0.588	0.560	0.672	0.044	0.056	0.056	0.712	0.608	0.560	
		Paired Beam	1	0	128	0.250	0.320	0.145	0.010	0.012	0.013	0.294	0.214	0.128
			2	2	132	0.352	0.554	0.410	0.010	0.020	0.016	0.444	0.318	0.244
			2	3	131	0.320	0.372	0.368	0.012	0.022	0.018	0.334	0.288	0.368
			2	4	130	0.166	0.492	0.044	0.046	0.054	0.057	0.278	0.296	0.278
			2	8	137	0.386	0.410	0.320	0.020	0.036	0.026	0.420	0.294	0.252
			2	9	136	0.296	0.238	0.410	0.024	0.028	0.024	0.268	0.318	0.338
			4	12	141	0.724	0.940	0.644	0.040	0.088	0.100	0.864	0.596	0.592
			4	13	142	0.536	0.568	0.476	0.032	0.040	0.040	0.544	0.428	0.448
			4	14	144	0.624	0.732	0.712	0.040	0.068	0.064	0.476	0.412	0.524
			4	15	140	0.764	1.060	0.824	0.056	0.056	0.072	0.976	0.840	0.764
			4	16	143	0.936	0.748	0.564	0.044	0.116	0.092	1.108	0.792	0.676
			4	22	152	0.972	0.744	0.780	0.052	0.092	0.084	1.244	0.840	0.632
			4	23	151	0.396	0.524	0.628	0.048	0.064	0.040	0.664	0.684	0.640
			4	24	150	0.716	0.788	0.684	0.040	0.072	0.084	0.544	0.472	0.548
			4	25	153	0.560	0.564	0.760	0.060	0.080	0.044	0.512	0.528	0.484

7 Summary

7.1 Uncertainty

The amplitude level of power density simulation is biased due to material property parameters and the internal configuration at mm Wave frequencies. Therefore, it is not possible to assign an exact uncertainty for the simulation results. However, for the RF exposure evaluation, simulation results were only used to select the highest worst-case beam ID for measurements. Power density results for measurement and simulation show similar results to justify the selection of the Beam ID used for measurements. All final power density evaluations were performed on a measurement system with uncertainty of approximately 1.5dB.